Available online at www.sciencedirect.com
ScienceDirect
Journal of the European Ceramic Society 31 (2011) 1451–1456
www.elsevier.com/locate/jeurceramsoc

Non-uniform ageing behavior of individual grain boundaries in ZnO varistor ceramics

Jinliang He *, Jun Liu, Jun Hu, Rong Zeng, Wangcheng Long

State Key Laboratory of Power Systems, Department of Electrical Engineering, Tsinghua University, Beijing 100084, China

Received 7 September 2010; received in revised form 12 January 2011; accepted 27 January 2011
Available online 23 February 2011

Abstract

In this paper, the ageing characteristics of individual grain boundaries in ZnO varistor ceramics were directly measured for the first time, which were carried out based on the microcontact technique in combination with accelerated AC voltage ageing tests. The current–voltage (*I–V*) characteristics of individual grain boundaries were measured on a microprobe station after the sample was degraded under different ageing time. The results indicated that the *I–V* characteristics of individual grain boundaries varied non-uniformly during ageing process, which could be roughly classified into two categories as monotonic and non-monotonic. It is revealed that degradation and recovery of electrical properties coexisted in the ageing process, which could be explained with ion migration and oxygen desorption mechanisms.

Keywords: ZnO varistor; Ageing characteristics; Individual grain boundary; Microcontact measurement; Non-uniformity

1. Introduction

ZnO varistor ceramics are polycrystalline *n*-type semiconductors which are mainly composed of ZnO material and other minor additives, such as Bi_2O_3, MnO_2, Sb_2O_3 and so on.[1–4] Owing to the formation of double-Schottky barrier around the grain boundary during sintering process, ZnO varistor behaves highly nonlinear current–voltage (*I–V*) characteristics and has been extensively studied in enhancing its nonlinearity, stability and pulse energy handling capability.[5–9] The stability of ZnO varistors, including long-term ageing characteristic and pulse degradation characteristic, is highly concerned with the life-span of these devices that have been widely used both in electronic and electrical systems against overvoltage surges. Generally, the ageing or the degradation of ZnO varistors may eventually lead to the deformation of double-Schottky barrier and deterioration in electrical property, and then result in protection failure.[10–13] Despite lots of previous studies have investigated the ageing or degradation characteristics of bulk ZnO varistor under AC, DC and pulse current or voltage stress, but rare ones debated on the variation of electrical property from the viewpoint of individual grain boundaries in microstructure scale, which is the origin of the nonlinear electrical properties for ZnO varistor ceramics.[14–19]

Up to now, several methods have been adopted to probe the electrical behavior of individual grain boundaries in ZnO varistors.[20–27] Van Kemenade and Eijnthoven measured the breakdown voltages on more than 500 grain boundaries by evaporating Au microelectrodes on the surface of ZnO samples and proposed that the average barrier voltage of single grain boundaries is around 3.6 V as the current through the grain boundary is 1 μA.[20] Tao et al. distinguished "good" and "bad" junction from the *I–V* curves of 50 single junctions by welding thin wires on the surface of ZnO varistor.[21] Olsson and Dunlop presented informative research to characterize the difference and symmetry of breakdown voltage for individual interfacial barriers using a complex microelectrode configuration.[22] They claimed that the junctions between ZnO and intergranular Bi_2O_3 exhibited asymmetric *I–V* characteristics with breakdown voltage of 3.2 V for one polarity and either 0.4 or 0.9 V for the other polarity. However, the interface between ZnO and pyrochlore was "inactive" and did not exhibit obvious nonlinearity. Sun et al. measured the electrical non-uniformity of grain boundaries within ZnO varistors and identified three types of grain boundaries with threshold voltage of 1.8 V, 3.5 V, and 6.0 V, respectively.[23] The percentages of these three types of grain boundaries were char-

* Corresponding author. Tel: +86 10 62775585; fax: +86 10 62784709.
E-mail address: hejl@tsinghua.edu.cn (J. L. He).

0955-2219/$ – see front matter © 2011 Elsevier Ltd. All rights reserved.
doi:10.1016/j.jeurceramsoc.2011.01.024

acterized and the results indicated that grain boundaries with threshold voltage of 3.5 V occupied dominant ratio (over 50%) within the varistors. Except for the *I–V* measurements, deep level transient spectroscopy (DLTS) and isothermal capacitance transient spectroscopy (ICTS) have also been performed based on microcontact technique to investigate the interface state levels of individual grain boundary of ZnO varistors by Wang and Tanaka, respectively.[24,25] Recently, Ramírez et al. adopted atomic force microscopy (AFM) and electrostatic force microscopy (EFM) to evaluate the charge distribution on varistor surface and the efficiency of the voltage barriers of ZnO varistor before and after pulse degradation.[26,27]

In this paper, we reported the ageing behavior of individual grain boundaries in ZnO varistor materials by microcontact measurement technique for the first time. Grain boundaries existing different ageing behaviors were distinguished and categorized. And then, the mechanism leading to such a non-uniform ageing behavior was analyzed in Section 4.

2. Experimental procedure

ZnO sample was prepared by conventional ceramic fabrication method. The content was 95.05 mol% ZnO, 0.70 mol% Bi_2O_3, 0.50 mol% MnO_2, 1.00 mol% Co_2O_3, 0.50 mol% Cr_2O_3, 1.00 mol% Sb_2O_3, and 1.25 mol% SiO_2. These analytical-grade reagents were homogenously mixed in a planetary mill, dried in an oven at 90 ° C and pressed under 160 MPa into discs with 20 mm in diameter and 2 mm in thickness. And then, the pellets were sintered at 1200 ° C for 4.5 h and polished to about 1.5 mm in thickness. Three varistor samples with the same composition and fabrication process were prepared. The following ageing test and microcontact measurement were carried out on these three samples at the same time. The results are similar, so only one of three samples is reported in this paper.

In order to perform the microcontact measurements on single ZnO grain boundaries, an array of Ag microelectrodes with 100 nm in thickness was evaporated on the polished surface of the ZnO sample by photolithography. The mean grain size of the sample was about 16.7 μm which was determined from the surface SEM graph illustrated in Fig. 1. Therefore, the electrode arrays were designed as 20 μm in diameter and 5 μm away from the adjacent electrodes for the convenience of microcontacts with microprobe and observation of individual grain boundaries.

And then, this ZnO sample was degraded under an accelerated AC voltage stress of 0.85 $V_{1\,mA}$ ($V_{1\,mA}$ correspond to the applied voltage at 1 mA) at 135 ° C for 3 ageing intervals (the accumulated ageing time is 0 h, 24 h and 48 h, respectively). Accordingly, the overall microcontact measuring experiments were divided into 3 stages and carried out after the accelerated ageing process is completed. A prominent mark was also made on the surface of sample so as to locate the same grain boundaries to be measured at different ageing stages.

Since the microelectrodes on the deposited side were isolated from each other, some parts of this side might not be well-conducted during the bulk electrical property measurements and ageing tests. An experimental setup, as shown in Fig. 2, was designed to eliminate the influence of poor surface contact. A lead plate was placed between the lower electrode and the deposition surface. The un-deposited regions on the deposited surface could be filled by lead because lead is very soft and could be deformed under pressure. As a result, both sides of the sample were firmly contacted with conductive materials, including the microelectrode array and sample surface.

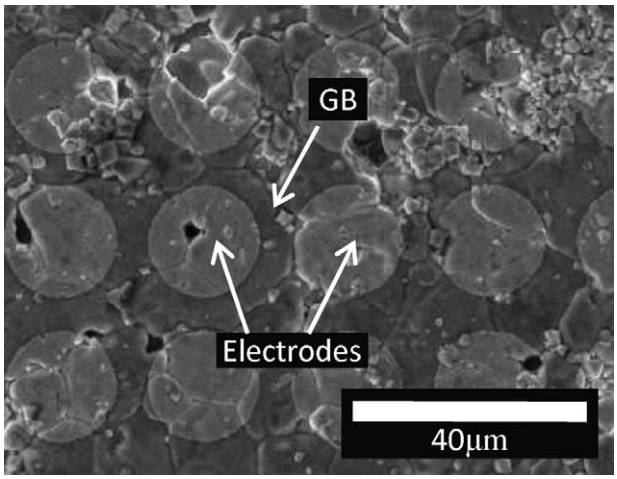

Fig. 1. Surface SEM image for ZnO ceramic sample coated with an array of round microelectrodes. Note that there may be zero, one, two, three or more grain boundaries located between the adjacent electrodes. For simplicity, we mainly focused on the electrode junctions containing only one grain boundary.

The microcontact measurements were performed on a probe station (Summit 11000M, Cascade Microtech Inc., Beaverton, OR, USA), an optical high magnification microscope (FS-70, Mitutoyo Corporation, Kawasaki-shi, Kanagawa, Japan), and a couple of coaxial probes with a 0.5 μm replaceable tip (DCP-105R, Cascade Microtech Inc., Beaverton, OR, USA) equipped with two probe positioners (DCM-320-M, Cascade Microtech Inc., Beaverton, OR, USA). The probes were manually manipulated by the positioners to make electrical contact with the deposited microelectrodes. And then, a digital source meter (Model 2410, Keithley Inc., Cleveland, OH, USA) was connected with the probes' coaxial cables to determine the *I–V* curves of individual grain boundaries.

The electrical property parameters of grain boundaries were derived from these measured *I–V* curves. For instance, the nonlinear coefficient was defined as the maximum of local nonlinear coefficients which were calculated by fitting the neighboring 5 data points logarithmically according to the equation $I = KV^{\alpha}$.

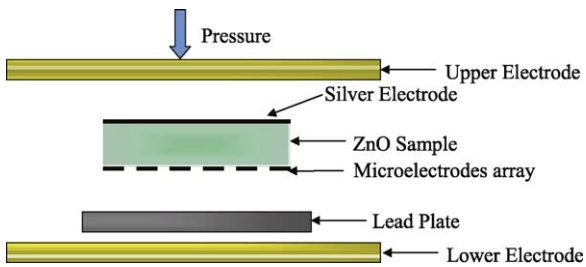

Fig. 2. The experimental setup for bulk electrical measurements and ageing tests.

And then, the applied voltage corresponding to this data point was defined as the breakdown voltage V_b of this grain boundary, while the current corresponding to 0.75 V_b was noted as the leakage current I_L. Additionally, the ageing rate coefficients K_T of single grain boundaries could be estimated by the empirical equation as follows:

$$I_L = I_{L0} + K_T t^{1/2} \quad (1)$$

where I_{L0} is the initial leakage current and I_L is the leakage current after stress, t is the ageing time.

3. Results and discussion

3.1. Microstructure of the sample's surface deposited with electrodes

The microstructure of ZnO ceramic sample coated with an array of microelectrodes is shown in Fig. 1. The round embossments on the surface are corresponding to the deposited Ag microelectrodes as marked by labels in Fig. 1. ZnO grains are surrounded by intergranular phase and spinel phase randomly distributed among the grain boundaries. Since these microelectrodes were deposited neatly and uniformly, there may be zero, one, two or more grain boundaries located in series between the adjacent microelectrodes. In order to simplify our discussions mainly on the ageing characteristics of single grain boundaries, microcontact measurements were restricted to carry out on the junctions with only one grain boundary. As reported by Olsson and Dunlop, different types of boundaries existed in ZnO varistor and had different electrical properties.[22] Boundaries between ZnO grains containing a thin intergranular amorphous Bi-rich film possessed a dominant portion in ZnO varistor sample and the breakdown voltages were about 3.2 V. ZnO grains separated by a layer of Bi_2O_3 and pyrochlore or spinels did not have obvious varistor behavior (low nonlinearity and low breakdown voltage), which were excluded from our study. Therefore, in our experiment, 25 junctions with breakdown voltage in the range from 3.0 V to 3.6 V were selected and labeled to investigate the variations in electrical properties under different ageing time. Once the accelerated ageing test was completed, the microcontact measurement on these 25 single grain boundaries were carried out subsequently.

3.2. The ageing characteristic of bulk ZnO varistor sample

Before carrying out the microcontact measurements on the sample's surface, the *I–V* characteristic curves of bulk ZnO varistor sample after different ageing times were measured, as well, and shown in Fig. 3. The pre-breakdown region of the *I–V* curve shifts towards the direction with current increasing as the ageing time accumulated, which means that obvious electrical degradation happens on this sample due to the accelerated AC voltage stress. The leakage current increases from 0.1 μA to 2.6 μA, while the nonlinear coefficient decreases from 43.4 to 38.6 when the total ageing time is 48 h.

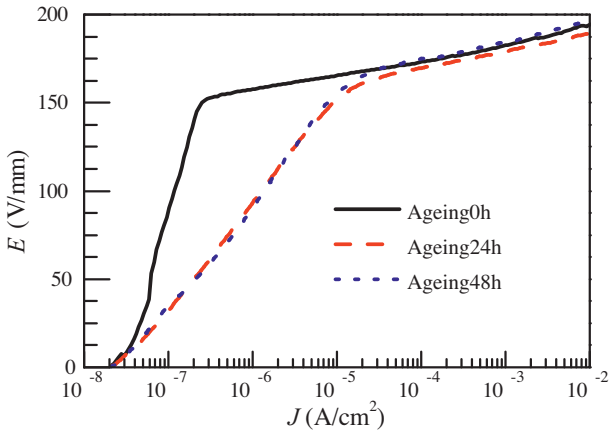

Fig. 3. The *I–V* characteristic curves of bulk ZnO sample at different ageing stage (0 h, 24 h and 48 h).

3.3. Non-uniformity in ageing behavior of individual grain boundaries

The *I–V* characteristic curves of 25 selected grain boundaries after different ageing time were measured to study the ageing characteristics of single grain boundaries in ZnO varistor ceramic. According to the variation trend of the leakage current in the pre-breakdown region, the ageing characteristics of individual grain boundaries can be distinguished and classified into two categories: monotonic and non-monotonic. Monotonic ageing process means that the leakage current of single grain boundary monotonously degrades at different ageing stage. On the contrary, non-monotonic ageing process means that some grain boundaries' leakage current could be recovered during the ageing process.

3.3.1. Grain boundaries exhibiting monotonic ageing behavior

A typical monotonic ageing process in *I–V* characteristic of single grain boundary is shown in Fig. 4. The breakdown voltage of this grain boundary is around 3.02 V. The pre-breakdown region and the breakdown region of the *I–V* characteristic curve gradually and monotonously move towards the direction

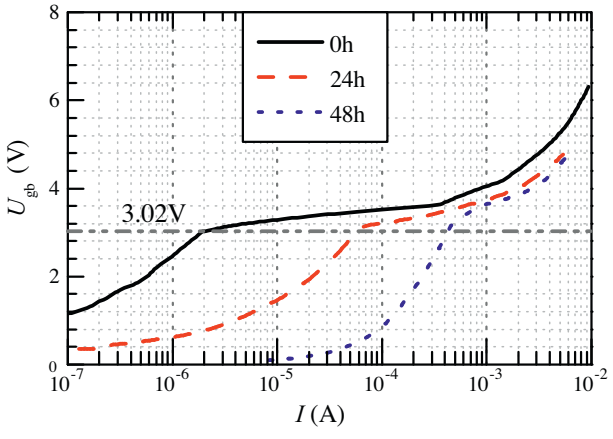

Fig. 4. A typical monotonic ageing process of a single grain boundary.

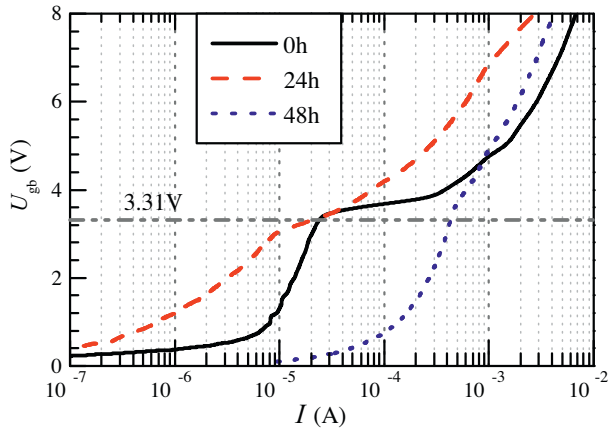

Fig. 5. Non-monotonic ageing process of a single grain boundary.

where the current increases. The leakage current increases from 91.9 nA to 1.63 μA, and then 4.06 μA, whereas the nonlinear coefficient decreases from 33.3 to 21.8, and then 4.2, when the ageing time increases. Meanwhile, the width of nonlinear breakdown region is significantly reduced after the sample was aged for 48 h. The degradation phenomenon of this grain boundary in the whole *I–V* curve is very noticeable and expected.

3.3.2. Grain boundaries exhibiting non-monotonic ageing behavior

A typical non-monotonic ageing process in *I–V* characteristic of single grain boundary is shown in Fig. 5. The breakdown voltage of this grain boundary is around 3.31 V. Since there is a recovery phenomenon in the pre-breakdown region of *I–V* curves after ageing 24 h, this ageing process differs a lot from that of Fig. 4. Even though, the trend of this ageing process tends to deteriorate in electrical properties, eventually. The leakage current decreases from 16.6 μA to 5.55 μA firstly, and then increases to 329 μA, whereas the nonlinear coefficient decreases from 17.1 to 8.8, and then 4.2, as the ageing time accumulated. Meanwhile, the width of the breakdown region is reduced after 48 h compared with its initial width.

3.3.3. Summary of the electrical properties of 25 individual grain boundaries at different ageing stage

The electrical properties of individual grain boundaries include the breakdown voltage, nonlinear coefficient and leakage current. Since the breakdown voltages after different ageing time basically remain constant in ageing process, the nonlinear coefficient and the leakage current are our primary concerned parameters. The nonlinear coefficients of 25 individual grain boundaries after different ageing times are summarized in Fig. 6. The initial nonlinear coefficients of these grain boundaries mainly distribute in the range from 25 to 40 and exhibit non-uniform variation. As the ageing time increases, the nonlinear coefficients of most grain boundaries gradually decrease. However, the decline degrees of different grain boundaries are greatly different among these grain boundaries. The nonlinear coefficients decrease very fast from their initial values when subjected to 24 h voltage stress. With the ageing test continuing, the decline

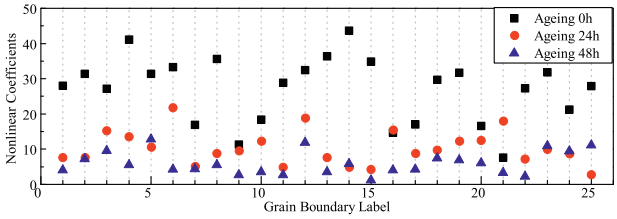

Fig. 6. The nonlinearities of 25 grain boundaries at different ageing stage.

Table 1
Mean value and standard deviation of the nonlinear coefficients and the leakage currents of the studied 25 individual grain boundaries at different ageing stage.

Ageing stage	Nonlinear coefficient		Leakage current in logarithmic format	
	Mean value	Standard deviation	Mean value	Standard deviation
0 h	27.1	9.3	−6.1	0.9
24 h	10.3	4.8	−4.6	1.3
48 h	6.0	3.3	−3.8	1.1

degrees of nonlinear coefficients of these selected grain boundaries at second ageing stage (ageing 48 h) are significant less than those obtained at the first ageing stage. After the sample was degraded 48 h, the nonlinear coefficients of individual grain boundaries are mainly distributed in the range from 5 to 10. The mean value and standard deviation of nonlinear coefficients of these 25 grain boundaries at different ageing stages are summarized in Table 1, which reveal the decline of nonlinearity in the ageing process intuitively.

The leakage currents of 25 individual grain boundaries after different ageing time are summarized in Fig. 7. The leakage currents of single grain boundaries before ageing test are in the range from 0.1 μA to 1 μA. As the ageing test time increased, different grain boundary behaves different ageing process, as mentioned above, including monotonic and non-monotonic process. The leakage currents of several grain boundaries exceed 1 mA after subjected to the voltage stress of 48 h, which is relatively large. Meanwhile, the corresponding nonlinear coefficient is very small, which means that the grain boundary becomes kind of "inactive" and has higher conductivity. In other words, these grain boundaries behave lower nonlinearity. 16 single grain boundaries of 25 investigated ones exhibit the monotonic ageing behavior, while the rest of them are non-monotonic. The mean value and the standard deviation of the leakage currents of these 25 grain boundaries at different ageing stages are summarized in Table 1, which directly reveal the leakage currents of grain boundaries increase in the ageing process directly.

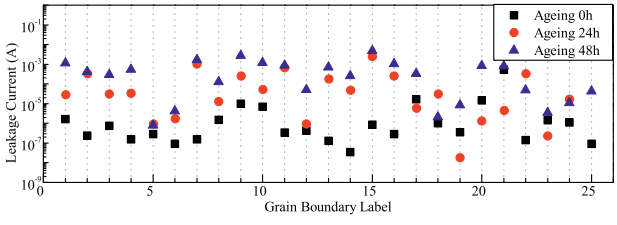

Fig. 7. The leakage currents of 25 grain boundaries at different ageing stage.

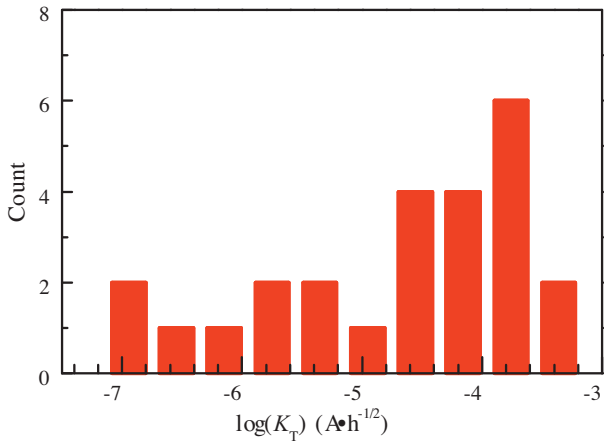

Fig. 8. The ageing rates distribution of 25 individual grain boundaries in the ZnO ceramic sample.

The ageing rate coefficients K_T of individual grain boundaries under 48 h accelerated ageing stress were calculated by Eq. (1), and then, the distribution of K_T could be summarized as shown in Fig. 8. Owing to the non-uniform ageing process of individual grain boundaries, the ageing rates of different grain boundaries are consequently non-uniform and range vastly from 10^{-7} to 10^{-3} A h$^{-1/2}$. It is expected that the ageing characteristic of bulk ZnO varistor sample is the synthetical effect of millions of individual grain boundaries with different ageing rates in a complicated network.

4. Discussions on the non-uniform ageing behavior

Totally, the samples with the same composition and fabrication process were prepared and tested, the grain boundaries' monotonic and non-monotonic ageing behaviors exist in all three samples. The proportions of monotonic to non-monotonic grain boundaries of these three samples are 16:9, 19:6 and 18:7, respectively. The actual mechanism that leads to the ageing phenomena of ZnO varistor is still on dispute. One of the main reasons is the lack of direct experimental support. The distribution of charged ions and defects in the depletion layer and boundary interface determine the double-Schottky barrier height. Generally, the ageing phenomenon of ZnO varistors is considered to be caused by the reduction of double-Schottky barrier height of individual grain boundary. There are mainly two mechanisms used to interpret the decline of the barrier height in the ageing process: interstitial ion migration and oxygen desorption.

A grain boundary defect model is widely accepted to describe the ion migration process.[28,29] Zinc interstitial ions in the depletion layer, which are considered to be the dominant migration ions, can move rapidly through the octahedral and half the tetrahedral interstitial sites in ZnO structure (Wurtzite form). Those positive ions migrate towards the negatively charged grain-boundary interface where charged defects are converted to neutral defects due to the following chemical reaction between defects:

$$Zn_i^{\bullet} + V'_{Zn} = Zn_i^{x} + V_{Zn}^{x} \quad (2)$$

As a result of these reactions at the interface, two neutral defects (Zn_i^x and V_{Zn}^x) are formed at the grain boundary interface to replace the charged ions ($Zn_i^{\bullet}$) and (V'_{Zn}). With the continuous ageing stress on the varistor, the barrier height declined continuously due to the loss of charged ions and the accumulation of neutral defects at the grain boundary interface.

Meanwhile, the desorption of oxygen in ZnO varistor plays an important role in the degradation process, this has been verified by Ramírez et al.[30,31] The tetragonal β-Bi_2O_3 phase in ZnO varistor is regarded as boundary activator to limit oxygen around the grain boundary, which is necessary to improve the barrier characteristics. The elimination of β-Bi_2O_3 phase in ZnO varistor after degradation stress would lead to the desorption of oxygen and deterioration of barrier.

Ion migration and oxygen desorption mechanism could be easily used to explain the monotonic ageing phenomenon in the single grain boundary ageing test. However, there are several grain boundaries (occupying an unignorable percentage in the randomly selected boundaries) exist non-monotonic ageing behavior. The *I–V* characteristic curves could be recovered after subjected voltage stress, which behave like the recovery phenomenon of bulk varistor samples under heat treatment in some extent. It means that there might be a counter mechanism on the *I–V* characteristic's variation of individual grain boundaries during the ageing tests. In our opinion, except for the migration of positively charged ions from depletion layer to the grain boundary interface, the migration of negatively charged defects from the grain boundary to the interface should also be taken into consideration. Although the major defects distributed in the grain boundaries which are spatially fixed at interfaces, the existence of extrinsic defects may migrate towards the interface under ageing stress and partly compensate the loss of negative charges at the interface, which results in the enhancement of barrier height in some extent. In addition, there could be an reversible process as compared to the desorption of oxygen, noted as absorption, which could improve the barrier property. The desorption and absorption of oxygen around the grain boundary may coexist in the ageing process. The barrier could be recovered when the absorption of oxygen possesses dominant ratio in the ageing process. The improvement of barrier height would eventually have an opposite effect on the deterioration of electrical properties, as noticed in Fig. 5. The above explanation is based on deduction, further detailed discussions on the non-monotonic ageing behavior will be conducted on specially prepared single grain boundary in the near future.

5. Conclusions

The ageing characteristics of individual grain boundaries in ZnO varistor ceramic has been studied based on microcontact technique and accelerated ageing test. The ageing behavior and ageing rates of single grain boundaries are found to be different from each other. Over 60% of investigated junctions have monotonic ageing process, while the rest have non-monotonic ageing process. It is suggested that the migration of zinc interstitials towards the interface at the grain boundaries and desorption of oxygen around the grain boundary lead to the degrada-

tion. However, the migration of negatively charged defects in grain boundaries towards the interface and absorption of oxygen should also be taken into consideration, which may lead to the recovery of electrical properties.

Acknowledgment

This work was supported by the National Natural Science Foundations of China under Grants 50425721 and 50737001.

References

1. Eda K. Zinc oxide varistors. *IEEE Electr Insul Mag* 1989;**5**(6):28–30.
2. Gupta TK. Application of zinc oxide varistors. *J Am Ceram Soc* 1990;**73**(7):1817–40.
3. Clarke DR. Varistor ceramics. *J Am Ceram Soc* 1999;**82**(3): 485–502.
4. Baudrier-Raybaut M, Haïdar R, Kupecek P, Lemasson P, Rosencher E. Random quasi-phase-matching in bulk polycrystalline isotropic nonlinear materials. *Nature* 2004;**432**(7015):374–6.
5. Leite ER, Varela JA, Longo E. Barrier voltage deformation of ZnO varistors by current pulse. *J Appl Phys* 1992;**72**(1):147–50.
6. Bueno PR, Leite ER, Oliveira MM, Orlandi MO, Longo E. Role of oxygen at the grain boundary of metal oxide varistors: a potential barrier formation mechanism. *Appl Phys Lett* 2001;**79**(1):48–50.
7. Erhart P, Albe K. Diffusion of zinc vacancies and interstitials in zinc oxide. *Appl Phys Lett* 2006;**88**(20):201918.
8. McKenna KP, Shluger AL. Electron-trapping polycrystalline materials with negative electron affinity. *Nat Mater* 2008;**7**(11):859–62.
9. Singh S, Rao MSR. Optical and electrical resistivity studies of isovalent and aliovalent 3*d* transition metal ion doped ZnO. *Phys Rev B* 2009;**80**(4):045210.
10. Lee W, Young RL. Defects and degradation in ZnO varistor. *Appl Phys Lett* 1996;**69**(4):526–8.
11. Tonkoshkur AS, Lyashkov AY, Gomilko IV, Ivanchenko AV. Effect of long-term electrical degradation on the distribution of donor impurities in ZnO varistor ceramics. *Inorg Mater* 2000;**36**(7):745–8.
12. Khanna R, Ip K, Heo YW, Norton DP, Pearton SJ, Ren F. Thermal degradation of electrical properties and morphology of bulk single-crystal ZnO surfaces. *Appl Phys Lett* 2004;**85**(16):3468–70.
13. Ramirez MA, Cilense M, Bueno PR, Longo E, Varela JA. Comparison of non-ohmic accelerated ageing of the ZnO- and SnO_2-based voltage dependent resistors. *J Phys D Appl Phys* 2008;**42**(1):015503.
14. Binks DJ, Grimes RW, Gupta TK. Incorporation of monovalent ions in ZnO and their influence on varistor degradation. *J Am Ceram Soc* 1993;**76**(9):2370–2.
15. Chen WP, Wang Y, Peng Z, Chan HLW. Degradation mechanism of ZnO ceramic varistors studied by electrochemical hydrogen charging. *Jpn J Appl Phys* 2003;**42**(1A–B):L48–50.
16. Barrado CM, Leite ER, Bueno PR, Longo E, Varela JA. Thermal conductivity features of ZnO-based varistors using the laser-pulse method. *Mater Sci Eng A-Struct Mater Prop Microstruct Process* 2004;**371**(1–2):377–81.
17. Chen WP, Chan HLW. Electroplating-induced degradation in ZnO ceramic varistors. *J Mater Sci* 2005;**40**(24):6593–6.
18. Wang MH, Hua KA, Zhao BY, Zhang NF. Degradation phenomena due to humidity in low voltage ZnO varistors. *Ceram Int* 2007;**33**(2):151–4.
19. Wang MH, Yao C, Zhang NF. Degradation characteristics of low-voltage ZnO varistor manufactured by chemical coprecipitation processing. *J Mater Process Technol* 2008;**202**(1–3):406–11.
20. van Kemenade JTC, Eijnthoven RK. Direct determination of barrier voltage in ZnO varistors. *J Appl Phys* 1979;**50**(2):938–41.
21. Tao M, Ai B, Dorlanne O, Loubiere A. Different "single grain junctions" within a ZnO varistor. *J Appl Phys* 1987;**61**(4):1562–7.
22. Olsson E, Dunlop GL. Characterization of individual interfacial barriers in a ZnO varistor material. *J Appl Phys* 1989;**66**(8):3666–75.
23. Sun HT, Zhang LY, Yao X. Electrical nonuniformity of grain boundaries with in ZnO varistors. *J Am Ceram Soc* 1993;**76**(5):1150–5.
24. Wang H, Li W, Cordaro JF. Single junctions in ZnO varistors studied by current–voltage characteristics and deep level transient spectroscopy. *Jpn J Appl Phys* 1995;**34**(4A):1765–71.
25. Tanaka A, Mukae K. ICTS measurements of single grain boundaries in ZnO:rare-earth varistor. *J Electroceram* 1999;**4**(S1):55–9.
26. Ramírez MA, Simões AZ, Márquez MA, Maniette Y, Cavalheiro AA, Varela JA. Characterization of ZnO-degraded varistors used in high-tension devices. *Mater Res Bull* 2007;**42**(6):1159–68.
27. Ramírez MA, Bassi W, Parra R, Bueno PR, Longo E, Varela JA. Comparative electrical behavior at low and high current of SnO_2 and ZnO-based varistors. *J Am Ceram Soc* 2008;**91**(7):2402–4.
28. Gupta TK, Carlson WG. A grain-boundary defect model for instability/stability of a ZnO varistor. *J Mater Sci* 1985;**20**(10):3487–500.
29. Leite ER, Varela JA, Longo E. A new interpretation for the degradation phenomenon of ZnO varistors. *J Mater Sci* 1992;**27**(19):5325–9.
30. Ramírez MA, Simões AZ, Bueno PR, Márquez MA, Orlandi MO, Varela JA. Importance of oxygen atmosphere to recover the ZnO-based varistors properties. *J Mater Sci* 2006;**41**(19):6221–7.
31. Marques VPB, Ries A, Simões AZ, Ramírez MA, Varela JA, Longo E. Evolution of $CaCu_3Ti_4O_{12}$ varistor properties during heat treatment in vacuum. *Ceram Int* 2007;**33**(7):1187–90.